SCIENTIFIC REPORTS

OPEN

Organic and inorganic carbon and their stable isotopes in surface sediments of the Yellow River Estuary

Received: 25 April 2018
Accepted: 6 July 2018
Published online: 17 July 2018

Zhitong Yu[1], Xiujun Wang[1], Guangxuan Han[2], Xingqi Liu[3] & Enlou Zhang[4]

Studying the carbon dynamics of estuarine sediment is crucial to understanding of carbon cycle in the coastal ocean. This study is to evaluate the mechanisms regulating the dynamics of organic (TOC) and inorganic carbon (TIC) in surface sediment of the Yellow River Estuary (YRE). Based on data of 15 surface sediment cores, we found that TIC (6.3–20.1 g kg^{-1}) was much higher than TOC (0.2–4.4 g kg^{-1}). Both TOC and TIC were generally higher to the north than to the south, primarily due to the differences in kinetic energy level (i.e., higher to the south). Our analysis suggested that TOC was mainly from marine sources in the YER, except in the southern shallow bay where approximately 75% of TOC was terrigenous. The overall low levels of TOC were due to profound resuspension that could cause enhanced decomposition. On the other hand, high levels of TIC resulted partly from higher rates of biological production, and partly from decomposition of TOC associated with sediment resuspension. The isotopic signiture in TIC seems to imply that the latter is dominant in forming more TIC in the YRE, and there may be transfer of OC to IC in the water column.

The rate of CO_2 build-up in the atmosphere depends on the rate of fossil fuel combustion and the rate of CO_2 uptake by the ocean and terrestrial biota. About half of the anthropogenic CO_2 has been absorbed by land and ocean. Large rivers that connect the land and ocean may play an important role in the global carbon cycle[1,2]. On the one hand, river can transport a significant amount of dissolved and particulate carbon materials from the land to the ocean, which are subject to recycling and sedimentation in the estuaries, or further transportation to the marginal seas[3,4]. On the other hand, there may be high levels of nutrients in the river waters, which could enhance biological uptake of CO_2 and subsequent carbon burial in the estuaries[5,6].

The Yellow River, the second longest river in China following the Yangtze River, provides approximately 50% of the freshwater discharged into the Bohai Sea every year[7]. There were some studies on sedimentary organic carbon around the Yellow River Estuary (YRE), which were mainly conducted in the Yellow River Delta[1,8,9] and in the shelf of the Bohai Sea[10–13]. Limited studies showed a large spatial variability (ranging from 0.7 to 7.7 g kg^{-1}) in total organic carbon (TOC) in the YRE[14], with the highest contribution (40–50%) of terrestrial organic carbon near the delta[11]. However, little is known about the TOC dynamics in the sediment for the transitional zone near the river mouth.

Limited studies of inorganic carbon dynamics have been conducted in the YRE. An earlier study showed that particulate inorganic carbon ($1.8\% \pm 0.2\%$) was significantly higher than particulate organic carbon ($0.5\% \pm 0.05\%$) in the water column of YRE[15]. A later analysis demonstrated that rate of $CaCO_3$ precipitation was modestly higher than rate of biological production in the water columns of the estuary[16]. These findings suggest that there might be more inorganic carbon (TIC) than TOC accumulated in the sediment of the YRE. However, there is no evidence to support it because little is known on the magnitude and variability of TIC in the YRE. On the other hand, recent studies have showed that there was a large amount of carbonate in the soils of lower part

[1]College of Global Change and Earth System Science, Beijing Normal University, Beijing, 100875, China. [2]Yantai Institute of Coastal Zone Research, Chinese Academy of Sciences, Yantai, Shandong, 264003, China. [3]College of Resource Environment and Tourism, Capital Normal University, Beijing, 100048, China. [4]State Key Laboratory of Lake Science and Environment, Nanjing Institute of Geography and Limnology, Chinese Academy of Sciences, Nanjing, 210008, China. Correspondence and requests for materials should be addressed to X.W. (email: xwang@bnu.edu.cn)

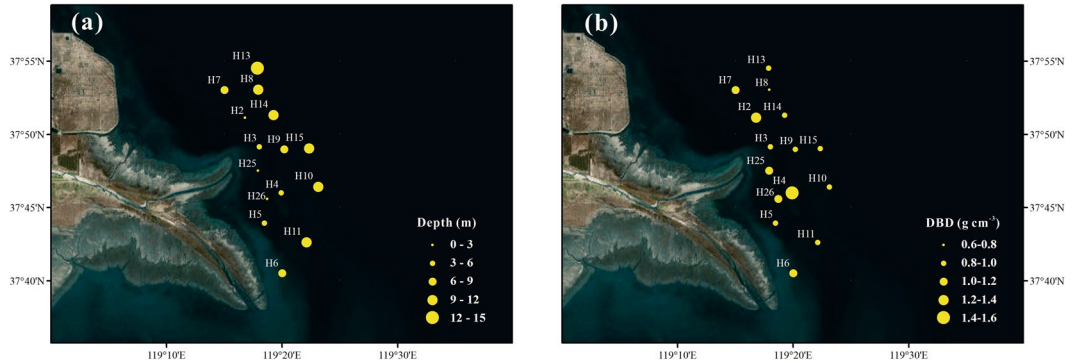

Figure 1. Spatial distributions of **(a)** depth (m) and **(b)** dry bulk density (DBD, g cm^{-3}) in surface sediments of the Yellow River Estuary. The maps were generated by ArcGIS 10.2 (http://www.esri.com/arcgis/about-arcgis).

of the Yellow River Basin, and higher level of carbonate was associated with high level of organic carbon[17,18]. One may expect a similar phenomenon in the sediment of the YRE.

As the world's largest carrier of fluvial sediment, the Yellow River's sediment load has continually decreased since the 1950s due to changes in water discharge and sediment concentration by anthropogenic changes[19]. On the other hand, climate change and human activities in the Yellow River basin have decreased fine sediment from the Loess Plateau and increased coarse sediment scouring from the lower river channel[20]. These changes may have profound impacts on the physical, biogeochemical and biological processes in the YRE. This study is the first to assess the dynamics of both TOC and TIC in the surface sediment of the YRE, focusing on the transitional zone near the river mouth[21]. The objective of this study is to test the hypothesis of more TIC than TOC accumulated in the sediment, and to explore the underlying mechanisms that regulate the variability of TOC and TIC in the YRE.

Results

Physical characteristics. The sampling sites covered most parts of the YRE, with water depth ranging from 1.5 m to 13.5 m (Fig. 1a). Dry bulk density (DBD) ranged from 0.74 to 1.55 g cm^{-3}, with an average of 1.02 g cm^{-3} (Table 1). Generally, DBD was much higher in the shallow water area than in the deep water region, presenting high values mainly occurred in the south and north sides near the river mouth (Fig. 1b).

Figure 2 showed the spatial distributions of the main granulometric variables of the surface sediment. In general, clay content was low, ranging from 1.4 to 10.8% (Table 1), with relatively higher values in the northern part than in the southern part. The highest clay content was found near the north side of the river mouth, and the lowest at the mouth section. Silt content was much high (69.4 ± 21.1%), exhibiting similar spatial distribution with clay. On the other hand, the highest content of sand was found at the mouth (Fig. 2c), where clay and silt contents were lowest (Fig. 2a,b). As expected, the spatial distribution of d(0.5) was similar to that of sand, displaying the highest values in the shallow river mouth section and lowest in the southern bay, indicating strong hydrodynamic effect in the former and weak in the latter.

Spatial distributions of TOC, TN, C:N and $\delta^{13}C_{org}$. Concentration of TOC was highly variable, with higher values (3.2–4.4 g kg^{-1}) in the northernmost section of the estuary and the east deep water area (Fig. 3a). There was also a high value of TOC in the bay, south of the river mouth. On the other hand, lower TOC concentration (0.2–1.4 g kg^{-1}) was observed in the south section. Similarly, TN value varied largely, from 0.06 to 0.68 g kg^{-1}, with the lowest at the shallow water area near the river mouth and the highest in the north deep water section (Fig. 3b). Overall, the spatial distribution of TN was similar to that of TOC, both showing higher values in the north and east deeper water area.

The C:N ratio ranged from 2.1 to 10.1 (Fig. 3c). In general, C:N ratio was higher in the shallow water part relative to the deep water part. The highest C:N ratio (8–10) was found in the southern bay, and the lowest in the shallow water area near the river mouth (<4.5). Figure 3d showed a considerable spatial variability in the $\delta^{13}C_{org}$ values with a range from −24.26‰ to −22.66‰. The $\delta^{13}C_{org}$ value was more negative near the river mouth and its adjacent south bay, and less negative far away from the river mouth and the coast line.

Spatial distribution of TIC, $\delta^{13}C_{carb}$ and $\delta^{18}O_{carb}$. There was a large spatial variation in TIC, as shown in Fig. 4a, ranging from 6.3 to 20.1 g kg^{-1}, with higher concentration in the northern deep sea area (>17 g kg^{-1}) away the mouth, and lower level in the south section (<13 g kg^{-1}). Apparently, TIC also presented a high value in the north and east part. Overall, the spatial distribution of TIC was similar to that of TOC. The values of $\delta^{13}C_{carb}$ and $\delta^{18}O_{carb}$ ranged from −4.89‰ to −3.74‰ and −10.92‰ to −7.92‰, respectively (Table 1). Generally, the spatial distribution of $\delta^{13}C_{carb}$ exhibited more negative values in the north and east deep sea area, which was opposite to that of $\delta^{18}O_{carb}$ (Fig. 4b,c).

		DBD	d0.5	Clay	F-Silt	M-Silt	C-Silt	Sand	TN	TOC	TIC	C:N	$\delta^{13}C_{org}$	$\delta^{13}C_{carb}$	$\delta^{18}O_{carb}$
		g cm^{-3}	μm	%					g kg^{-1}				‰		
Sediment	Mean	1.02	34.2	6.1	34.8	13.7	20.9	24.5	0.36	2.3	14.1	6.3	−23.35	−4.36	−8.92
	SD	0.20	26.3	2.9	19.0	6.7	9.4	23.8	0.19	1.3	4.0	1.7	0.48	0.41	0.90
	CV	0.20	0.77	0.47	0.55	0.49	0.45	0.97	0.53	0.57	0.28	0.27	−0.02	−0.09	−0.10
Wetland Soil	Mean	/	28.2	4.7	31.1	25.8	25.8	12.5	0.77	8.9	12.9	10.8	−22.5	−4.0	−9.1
	SD	/	15.8	1.2	15.5	9.3	10.4	15.1	0.55	8.0	4.8	3.0	3.4	0.72	0.62
	CV	/	0.56	0.26	0.50	0.36	0.40	1.21	0.71	0.90	0.37	0.27	−0.15	−0.18	−0.07

Table 1. Means, standard deviation (SD) and coefficients of variation (CV) of the main variables. Clay: <2 μm, F-Silt: 2–16 μm, M-Silt: 16–32 μm, C-Silt: 32–64 μm, Sand: >64 μm; C:N: TOC:TN.

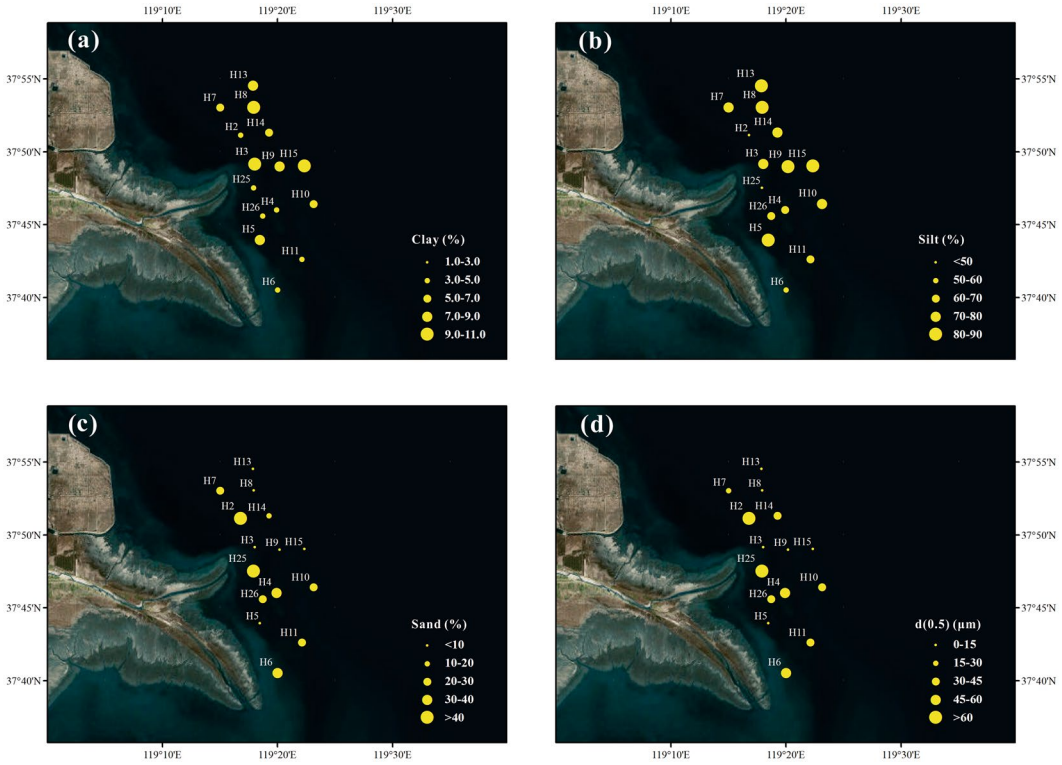

Figure 2. Distributions of **(a)** clay (%), **(b)** silt (%), **(c)** sand (%), **(d)** the median diameter (d(0.5), μm) in surface sediments of the Yellow River Estuary. The maps were generated by ArcGIS 10.2 (http://www.esri.com/arcgis/about-arcgis).

Discussion

Sources for TOC in the Yellow River Estuary. It is well known that human activities such as industrial and agricultural development would cause an increase in riverine input of nutrients and organic materials, leading to enhancements in estuary productivity and TOC burial in the sediment[22–24]. There was evidence that $\delta^{13}C_{org}$ was less negative in the central Bohai Sea (−21‰ to −22‰) than in the nearshore (~−27‰)[11], indicating more negative $\delta^{13}C_{org}$ in terrigenous OC. Provided that the $\delta^{13}C_{org}$ values ranged from −24.26‰ to −22.66‰, organic carbon in surface sediment of the YRE might be mainly from marine sources.

Since C:N ratio is significantly smaller in marine particles than in terrestrial organic matters, one may use a two-end-member mixing model to quantify different sources of OC; such approach has been widely applied in studies of wetland and lake sediments[25–27], and offshore and marine sediments[28,29]. Given that TOC:TN ratio was lower than 5.5 g:g at some sites in the YRE, it was reasonable to assume that there were terrestrial inputs of inorganic nitrogen. There was a significant corelation between TN and TOC (Fig. 5a), with an intercept of 0.0297 g N kg^{-1}. Following Schubert and Calvert[30], we calculated total organic nitrogen (TON) concentration of each sample by subtracting 0.0297 g N kg^{-1} (the intercept) from TN. As shown in Table 2, TOC:TON ratio was low (<7.1) in most sections, illustrating that TOC was mainly autochthonous in the surface sediment the YRE. On the other hand, mean TOC:TON ratio was 9.5 in the southern shallow bay; such high C:N ratio together with relatively more negative $\delta^{13}C_{org}$ value (Table 2) suggested that there might be a large amount of allochthonous OC sources in this section.

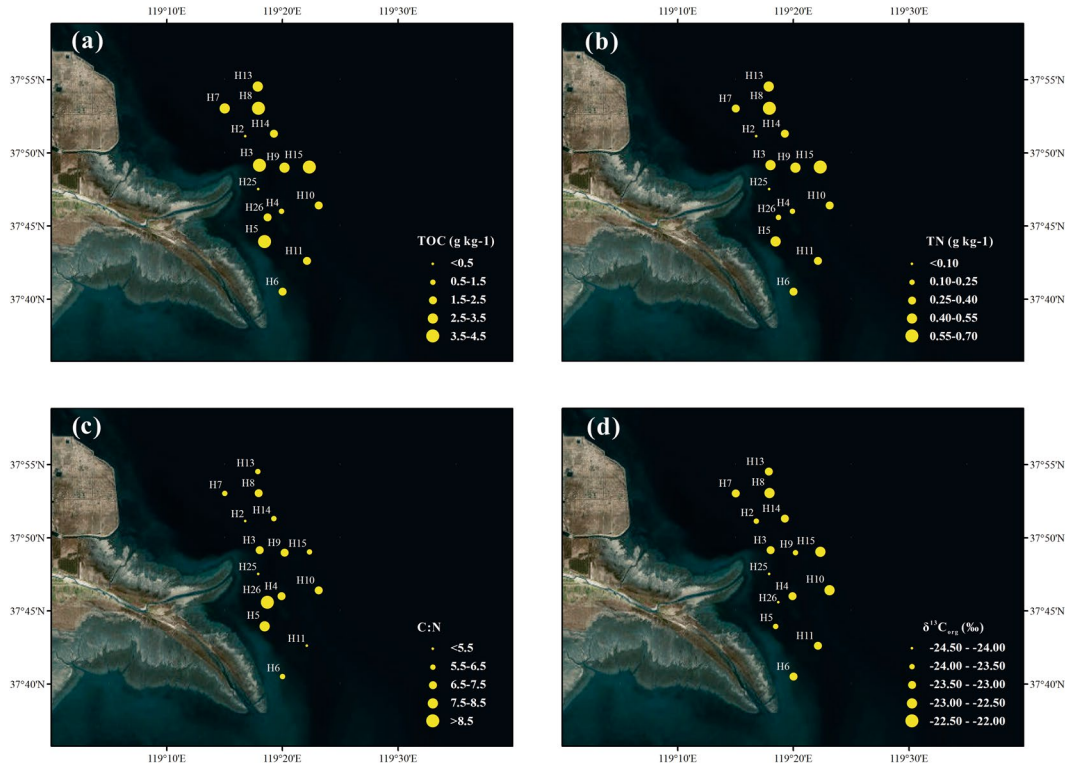

Figure 3. Spatial distributions of **(a)** TOC (g kg^{-1}), **(b)** TN (g kg^{-1}), **(c)** C:N, **(d)** $\delta^{13}C_{org}$ (‰) in surface sediments of the Yellow River Estuary. The maps were generated by ArcGIS 10.2 (http://www.esri.com/arcgis/about-arcgis).

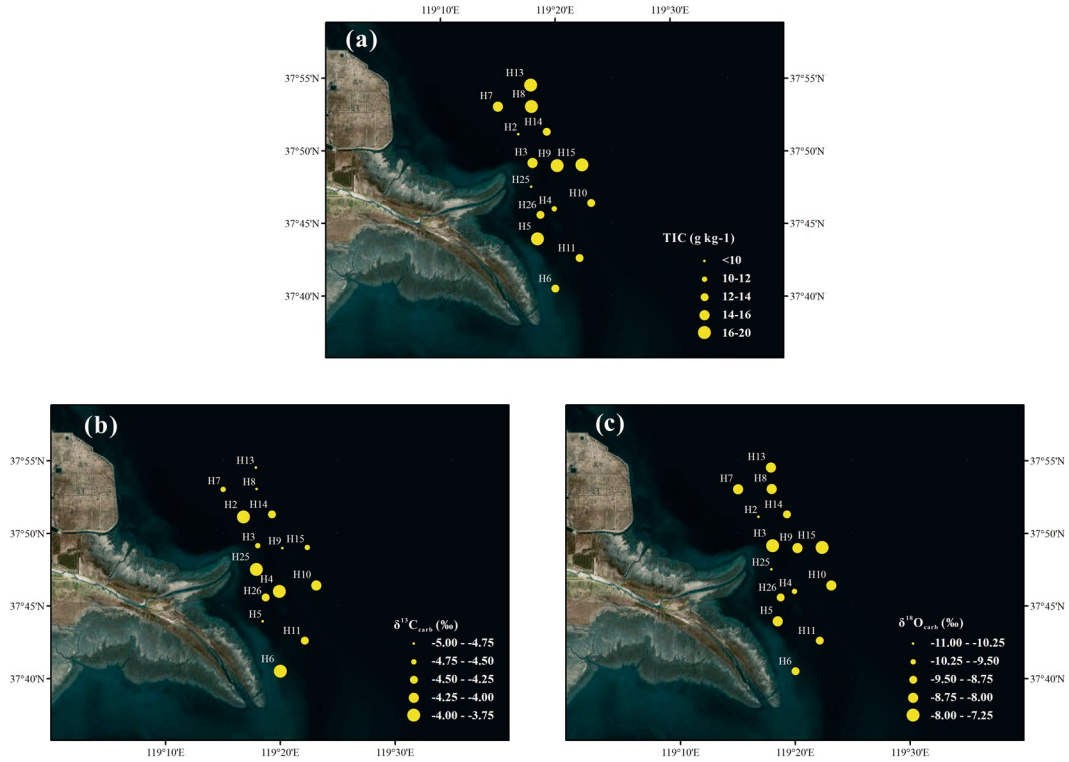

Figure 4. Spatial distributions of **(a)** TIC (g kg^{-1}), **(b)** $\delta^{13}C_{carb}$ (‰), and **(c)** $\delta^{18}O_{carb}$ (‰) in surface sediments of the Yellow River Estuary. The maps were generated by ArcGIS 10.2 (http://www.esri.com/arcgis/about-arcgis).

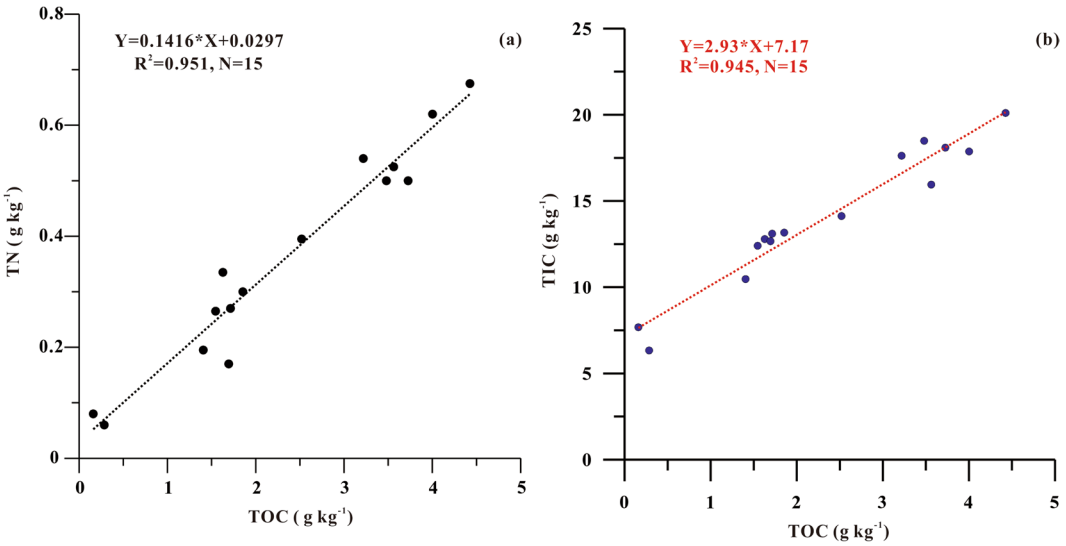

Figure 5. Relationship between **(a)** TOC and TN, **(b)** TOC and TIC in surface sediments of the Yellow River Estuary.

Section	Depth (m)	DBD (g cm^{-3})	d(0.5) (μm)	TN (g kg^{-1})	TOC (g kg^{-1})	TIC (g kg^{-1})	TOC/TON	$\delta^{13}C_{org}$ (‰)	$\delta^{13}C_{carb}$ (‰)	$\delta^{18}O_{carb}$ (‰)
North	10.8	0.88	20.2	0.47	3.0	16.2	6.8	−23.11	−4.70	−8.55
South	8.9	1.02	41.4	0.30	1.7	12.8	6.3	−23.04	−4.09	−8.96
Center	8.1	0.92	10.5	0.55	3.7	17.4	7.1	−23.15	−4.64	−8.03
Bay	3.5	1.21	33.4	0.29	2.3	13.7	9.5	−23.71	−4.31	−9.00

Table 2. Means of the variables in different sections. North: H7, H8, H13, H14; South: H6, H10, H11; Center: H3, H9,H15; Bay: H4, H5, H26.

	$Soil_{C:N} = 10.8^A$		$Soil_{C:N} = 9.5^B$		$Soil_{C:N} = 13.4^C$	
Section	Marine	Terrestrial	Marine	Terrestrial	Marine	Terrestrial
North	78	22	70	30	85	15
South	88	12	84	16	92	8
Center	72	28	62	38	81	19
Bay	25	75	0	100	50	50

Table 3. Relative contributions (%) of marine and terrestrial sources using different soil C:N ratios as the end-member. A, B and C presented the soil C:N in our study, in the lower Yellow River Basin and in the Chinese Loess Plateau, respectively.

To quantify the relative contributions of autochthonous and allochthonous OC in the surface sediments, we applied a two-end-member mixing model by using TOC:TON ratio, and assuming 6.6 mol:mol as the marine end-member. Using the average C:N ratio (10.8 g:g) from the soils collected near the river mouth (Table 1), we estimated that 75% of TOC was from soil OC source in the bay section, but only 12–28% in other sections of the YRE (Table 3). However, our approach could introduce bias or uncertainty due to the choice of end member value for soil C:N ratio. According to our recent study[31], soil C:N ratio varied from 9.5 to 13.4 in the middle-lower parts of Yellow River Basin. If we chose 9.5 (or 13.4) as the soil C:N end member, the terrigenous contribution would be increased (or decreased) by 4–25%. Nevertheless, TOC in the surface sediment was primarily autochthonous in most parts of the YRE.

TOC variability in the Yellow River Estuary. The magnitude and spatial distribution of TOC in estuarine sediment may reflect multiple and complex processes[10,32]. As shown in Fig. 2, the surface sediments were finer to the north than to the south. In general, coarser (finer) sediment particles usually indicated a stronger (weaker) water energy environment[33,34]. These analyses indicated that the relatively lower TOC values in the south section were attributable to higher kinetic energy level. On the other hand, a significantly positive relationship ($r = 0.71$, $p < 0.01$) between the $\delta^{13}C_{org}$ value and water depth (Table 4) implied that the shallow sections in the YRE accumulated more terrigenous OC (with more negative $\delta^{13}C_{org}$ values).

	Depth	DBD	d0.5	Clay	Silt	Sand	TOC	TIC	$\delta^{13}C_{org}$	$\delta^{13}C_{carb}$
TOC	0.54*	−0.65**	−0.94**	0.97**	0.88**	−0.90**		0.97**	0.50	−0.90**
TIC	0.63*	−0.70**	−0.96**	0.93**	0.93**	−0.94**	0.97**		0.47	−0.93**
$\delta^{13}C_{org}$	0.71**	−0.37	−0.55*	0.55*	0.53*	−0.54*	0.50	0.47		−0.32
$\delta^{13}C_{carb}$	−0.54*	0.73**	0.90**	−0.88**	−0.85**	0.87**	−0.90**	−0.93**	−0.32	
$\delta^{18}O_{carb}$	0.63*	−0.65**	−0.98**	0.94**	0.96**	−0.97**	0.91**	0.93**	0.63*	−0.84**

Table 4. Correlation coefficient (r) between various variables for the sediments. Significance of Pearson correlation is marked with one ($p < 0.05$) and two ($p < 0.01$) superscripts.

There is evidence that the magnitude and variability of OC is largely influenced by primary productivity, followed by sediment resuspension and riverine input in the Yellow-Bohai Sea[35]. In general, an increase of water productivity would cause enriched ^{13}C in carbonate[36,37]. However, we found a significantly negative correlation ($p < 0.01$, Table 4) between TOC and $\delta^{13}C_{carb}$ in the YRE, indicating that higher levels of TOC (with more negative $\delta^{13}C_{carb}$) were not a result of local biological production. Given that sediment resuspension played a large role in regulating the spatial-temporal variability of POC in the Yellow-Bohai Sea[35,38], we inferred that the current system would cause re-distribution of POC thus TOC in the surface sediment. Therefore, more OC could deposit in the north and east deep water area (with lower kinetic energy levels) in the YRE.

Dynamics of TIC and underlying mechanisms. Concentration of TIC in the surface sediment of the YRE was relatively higher in the north section (16.2 g kg^{-1}) than in the south section (12.8 g kg^{-1}) (Table 2), which was consistent with TOC. As shown in Fig. 5b, there was a significantly positive correlation between TOC and TIC in the surface sediments in the YRE ($r = 0.97$, $p < 0.01$), implying a potential relationship between the two parameters. In general, OC production (i.e., uptake of CO_2) can induce changes of chemical properties in the water column, which often leads to precipitation of carbonate[36,37,39]. Our analyses showed that the change ratio between TIC and TOC (i.e., the slope of 2.93 in Fig. 5b) in the surface sediment of the YRE was close to the ratio of 3.6 for IC:OC in particles in the water column by Gu, *et al.*[15], indicating that the spatial variability of TIC might be driven by variability of POC.

While higher levels of TIC might be associated with higher levels of TOC, there was a big intercept (7.17 in Fig. 5b) for the TIC-TOC relationship in the surface sediment, suggesting that there were other processes of $CaCO_3$ formation, which were not linked with biological production. If higher levels of TIC were a result of higher rates of biological production, one would expect an enrichment of ^{13}C in carbonate; on the other hand, higher rate of respiration/decomposition would lead to depleted ^{13}C in dissolved IC thus in carbonate[36,37]. The significantly negative relationship ($p < 0.01$) between $\delta^{13}C_{carb}$ and TIC in the YRE (Table 4) indicated that higher levels of TIC (with more negative $\delta^{13}C_{carb}$) might result from high rates of decomposition of OC. Given that both TIC and TOC had a significantly negative correlation ($p < 0.01$, Table 4) with $\delta^{13}C_{carb}$ in the YRE, we speculated that there might be decomposition of TOC/POC associated with sediment resuspension, which would lead to an increase in dissolved IC thus promote carbonate precipitation and sedimentation.

Comparisons with other studies. There have been many studies of TOC but only a few studies of TIC from the estuarine sediments. Overall, TOC levels are lower in the surface sediments in most estuaries in China, relative to those in the South and Southeast Asia[40,41], Europe[42,43], North America and South America[44,45]. In general, sedimentary TOC concentration is relatively lower in large river estuaries (e.g., the Yangtze River Estuary[46,47] and Pearl River Estuary[48,49]) than in small river estuaries (e.g., the Luan River Estuary[50], Licun Estuary[51], Min River Estuary[52] and GQ Estuary[53]), which indicating that weak hydrodynamic environment (in the small estuaries) was beneficial to accumulation of organic carbon[11,54].

For the surface sediment near the river mouth in the YRE, TOC concentration was modestly lower in our study (0.2 to 4.4 g kg^{-1}) than the previous reports of 0.7–7.7 g kg^{-1} [14] and <1 to 6.0 g kg^{-1} [11], which may be attributable to the decline in the Yellow River's discharge over the past decade[19]. On the other hand, TOC levels near the Yellow River's mouth were significantly lower than those in the other coastal areas of the Bohai Sea, e.g., north off the YRE (2.6–17.2 g kg^{-1})[55] and the Laizhou Bay (5.7–12.8 g kg^{-1})[13], which may reflect the different influences of kinetic energy level and terrigenous inputs.

The surface sediments contained much lower TOC in the YRE than other large estuaries in China (i.e., Yangtze River Estuary[46,47] and Pearl River Estuary[48,49]). Interestingly, the primary productivity in the YRE was higher than that in the Yangtze River Estuary[56,57]. On the other hand, our recent study indicated that POC in the Yellow River Estuary was comparable to that in the Yangtze River Estuary, and there was profound, nearly year-around sediment resuspension in the Yellow-Bohai Sea particularly in the shallow sections[38], implying that surface sediment was subject to frequent disturbing, transportation and recycling thus decomposition, which might be partly responsible for the lower TOC levels in the YRE.

However, the YRE had much higher TIC values than those (3.3–8.2 g kg^{-1}) in the Cochin Estuary[40], Vellar and Coleroon Estuary[58], and Chilika Lagoon[41] of the South Asia. The large difference may be attributable to factors such as water quality, net biological production and respiration, and sediment resuspension processes[59–61]. For example, the conditions with rich calcium and magnesium ions and strong water exchange between salty and fresh waters would lead to much more carbonate precipitation in the YRE[13,16].

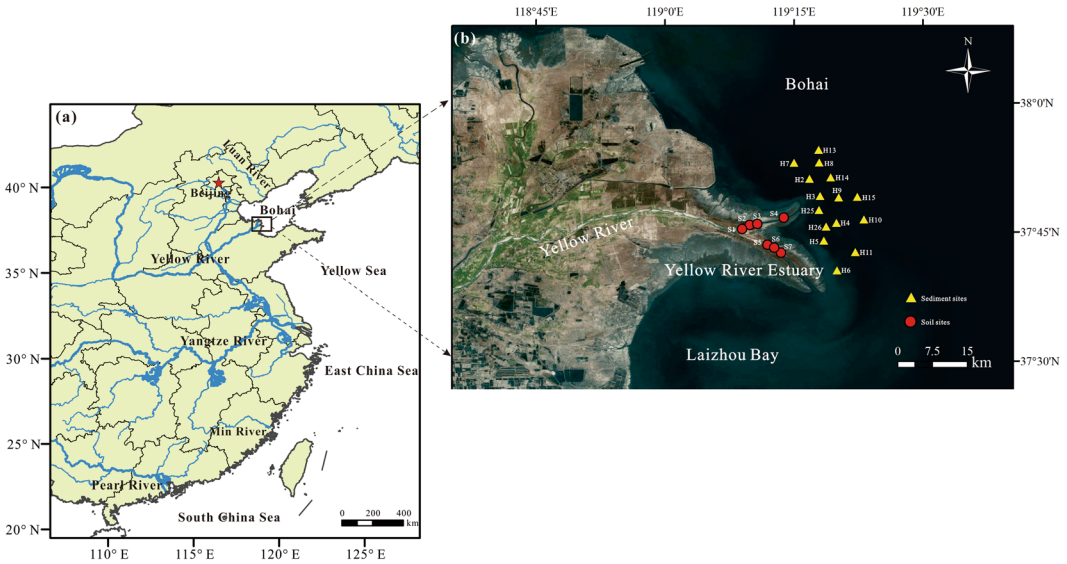

Figure 6. Map of **(a)** the large Chinese river-estuarine systems and **(b)** the Yellow River Estuary with the sampling sites. The figure was generated using ArcGIS 10.2 software (http://www.esri.com/arcgis/about-arcgis).

Conclusions and Implications

To our best of knowledge, this study is the first to evaluate both TOC and TIC in the surface sediment of the YRE, and to explore the underlying processes determining the dynamics of TOC and TIC. We found that TIC concentration (6.3–20.1 g kg^{-1}) was much higher than TOC (0.2–4.4 g kg^{-1}), and both TOC and TIC were higher to the north (3.0 and 16.2 g kg^{-1}) than to the south (1.7 and 12.8 g kg^{-1}). The relatively lower TOC and TIC values in the south section were attributable to higher kinetic energy level. Our analyses indicate that TOC in surface sediment are mainly autochthonous except in the southern bay where approximately 75% of TOC is probably from terrigenous OC. Overall low levels of TOC in the surface sediment of YER are mainly due to the profound resuspension that can cause enhanced decomposition. On the other hand, higher levels of carbonate in surface sediment of the YRE result partly from higher rate of biological production, and partly from decomposition of POC/TOC associated with sediment resuspension. The isotopic signiture in TIC seems to imply that the latter is dominant in forming more TIC in the YRE, and there may be transfer of OC to IC in the water column. Further studies with integrative and quantitative approaches are needed not only to assess the spatial and temporal variations of major carbon forms in the water column and sediments, but also to quantify the contributions of various sources and transformations among the different carbon pools, which aims to better understand the carbon cycle in the YRE in the changing environment.

Materials and Methods

Site description. The YRE is a typical river-dominated estuary with weak tides, where has a warm-temperate continental monsoon climate with distinct seasons (Fig. 6). In the YRE, monthly water temperature is 4.1 °C in January and 26.7 °C in July, and annual wind speed ranges from 3.1 to 4.6 m s^{-1} in the estuary[62]. The estuary is characterized by a high sediment load (mainly composed of silt) in the water column, produced largely by the erosion from the China's Loess Plateau. Most of the sediments discharged from the modern Yellow River mouth are trapped in the subaqueous delta or within 30 km of the delta front by gravity-driven underflow[9,63]. In recent decades, the annual water and sediment fluxes have declined dramatically, which is caused by regional climate change, reservoir construction, and irrigation-related withdrawals[16,19,62].

Field sampling and analyses. During October 2016, we collected 15 short sediment cores (H series) from the YRE using a Kajak gravity corer and 10 surface soil samples at 7 sites (S1–S7) along its upstream wetland (Fig. 6b). Each sediment core was carefully extruded and cut into 1-cm interval in the filed, and then placed in polyethylene bags which were kept on ice in a cooler during transport. In the laboratory, we took the top 2 cm sediment and surface soil samples, and then freeze-dried for 48 h before analyses.

Grain size was determined using a Malvern Mastersizer 2000 laser grain size analyzer. According to Yu *et al.* (2015), each sediment sample and soil sample (~0.5 g) was pretreated, in a water bath (at 60–80 °C), with 10–20 ml of 30% H_2O_2 to remove organic matter, and with 10–15 ml of 10% HCl to remove carbonates. The pretreated samples were then mixed with 2000 ml of deionized water, and centrifuged after 24 hours of standing. The solids were dispersed with 10 ml of 0.05 M $(NaPO_3)_6$, and then analyzed for grain size (between 0.02 and 2000 μm). The Malvern Mastersizer 2000 automatically outputs the median diameter d(0.5) (μm), the diameter at the 50th percentile of the distribution, and the percentages of clay (<2 μm), silt (2–64 μm) and sand (>64 μm) fractions.

Elemental analysis was measured using an Elemental Analyzer 3000 (Euro Vector, Italy) at the State Key Laboratory of Lake Science and Environment, Nanjing Institute of Geography and Limnology, Chinese Academy of Sciences. Freeze-dried samples were ground into a fine powder, then placed in tin capsules, weighed and packed carefully. For the analysis of TOC/soil OC, a ~0.3 g sample was pretreated with 5–10 ml 2 M HCl for 24 h

at room temperature (to remove carbonate), and followed by washing with deionized water then drying overnight at 40–50 °C. Total carbon (TC) and total nitrogen (TN) were analyzed without pretreatment of HCl, and TIC/soil IC was calculated as the difference between TC and TOC/soil OC.

For the analyses of ^{13}C in TOC/soil OC ($\delta^{13}C_{org}$), approximately 0.2 g of the freeze-dried sample was pretreated with 5–10 ml 2 M HCl for 24 h at room temperature to remove carbonate, and then mixed with deionized water to bring the pH to 7, and dried at 40–50 °C before analyses. Each pre-treated sample was combusted in a Thermo elemental analyzer integrated with an isotope ratio mass spectrometer (Delta Plus XP, Thermo Finnigan MAT, Germany). Additionally, ^{13}C and ^{18}O in carbonate ($\delta^{13}C_{carb}$ and $\delta^{18}O_{carb}$) were measured following reaction with 100% phosphoric acid on a stable isotope ratio mass spectrometer (Thermo-Fisher MAT 253, Germany), at the Nanjing Institute of Geology and Paleontology, Chinese Academy of Sciences. All the isotope data were reported in the conventional delta notation relative to the Vienna Pee Dee Belemnite (VPDB). Analytical precision was 0.1‰ for $\delta^{13}C_{org}$ and $\delta^{13}C_{carb}$, and 0.2‰ for $\delta^{18}O_{carb}$.

Statistical methods and mapping. The p-value from the correlation analysis was derived from functions in SPSS statistics software (version 19, IBM, USA). A Pearson-test analysis was performed to determine the correlation's significance. Spatial distribution maps were generated by ArcGIS 10.2 software (http://www.esri.com/arcgis/about-arcgis).

References

1. Bianchi, T. S. & Allison, M. A. Large-river delta-front estuaries as natural "recorders" of global environmental change. *Proceedings of the National Academy of Sciences* **106**, 8085–8092 (2009).
2. Ran, L. *et al*. CO2 outgassing from the Yellow River network and its implications for riverine carbon cycle. *Journal of Geophysical Research Biogeosciences* **120**, 1334–1347 (2015).
3. Cole, J. J. *et al*. Plumbing the Global Carbon Cycle: Integrating Inland Waters into the Terrestrial Carbon Budget. *Ecosystems* **10**, 172–185, https://doi.org/10.1007/s10021-006-9013-8 (2007).
4. Bauer, J. E. *et al*. The changing carbon cycle of the coastal ocean. *Nature* **504**, 61–70, https://doi.org/10.1038/nature12857 (2013).
5. Cai, W. J. Estuarine and Coastal Ocean Carbon Paradox: CO2 Sinks or Sites of Terrestrial Carbon Incineration? *Annual Review of Marine Science* **3**, 123–145, https://doi.org/10.1146/annurev-marine-120709-142723 (2010).
6. Raimonet, M. & Cloern, J. E. Estuary–ocean connectivity: fast physics, slow biology. *Global Change Biology* **23**, 2345–2357 (2017).
7. Wang, H., Yang, Z., Saito, Y., Liu, J. P. & Sun, X. Interannual and seasonal variation of the Huanghe (Yellow River) water discharge over the past 50 years: Connections to impacts from ENSO events and dams. *Global and Planetary Change* **50**, 212–225, https://doi.org/10.1016/j.gloplacha.2006.01.005 (2006).
8. Ye, S. *et al*. Carbon Sequestration and Soil Accretion in Coastal Wetland Communities of the Yellow River Delta and Liaohe Delta, China. *Estuaries and Coasts* **38**, 1885–1897, https://doi.org/10.1007/s12237-014-9927-x (2015).
9. Zhao, G., Ye, S., Li, G., Ding, X. & Yuan, H. Late Quaternary Strata and Carbon Burial Records in the Yellow River Delta, China. *Journal of Ocean University of China* **14**, 446–456, https://doi.org/10.1007/s11802-015-2773-z (2015).
10. Hu, L. *et al*. Recent organic carbon sequestration in the shelf sediments of the Bohai Sea and Yellow Sea, China. *Journal of Marine Systems* **155**, 50–58, https://doi.org/10.1016/j.jmarsys.2015.10.018 (2016).
11. Liu, D., Li, X., Emeis, K.-C., Wang, Y. & Richard, P. Distribution and sources of organic matter in surface sediments of Bohai Sea near the Yellow River Estuary, China. *Estuarine, Coastal and Shelf Science* **165**, 128–136, https://doi.org/10.1016/j.ecss.2015.09.007 (2015).
12. Xing, L., Hou, D., Wang, X., Li, L. & Zhao, M. Assessment of the sources of sedimentary organic matter in the Bohai Sea and the northern Yellow Sea using biomarker proxies. *Estuarine, Coastal and Shelf Science* **176**, 67–75, https://doi.org/10.1016/j.ecss.2016.04.009 (2016).
13. Wang, Y. *et al*. Distribution and source identification of trace metals in the sediment of Yellow River Estuary and the adjacent Laizhou Bay. *Physics and Chemistry of the Earth, Parts A/B/C* **97**, 62–70, https://doi.org/10.1016/j.pce.2017.02.002 (2017).
14. Li, L., Wang, X., Zhu, A., Yang, G. & Liu, J. Assessing metal toxicity in sediments of Yellow River wetland and its surrounding coastal areas, China. *Estuarine, Coastal and Shelf Science* **151**, 302–309, https://doi.org/10.1016/j.ecss.2014.07.010 (2014).
15. Gu, D., Zhang, L. & Jiang, L. The effects of estuarine processes on the fluxes of inorganic and organic carbon in the Yellow River estuary. *Journal of Ocean University of China* **8**, 352–358, https://doi.org/10.1007/s11802-009-0352-x (2009).
16. Liu, Z. *et al*. Removal of dissolved inorganic carbon in the Yellow River Estuary. *Limnology and Oceanography* **59**, 413–426 (2014).
17. Guo, Y. *et al*. Dynamics of soil organic and inorganic carbon in the cropland of upper Yellow River Delta, China. **6**, 36105, https://doi.org/10.1038/srep36105 (2016).
18. Shi, H. J. *et al*. Relationship between soil inorganic carbon and organic carbon in the wheat-maize cropland of the North China Plain. *Plant and Soil*, https://doi.org/10.1007/s11104-017-3310-1 (2017).
19. Wang, S. *et al*. Reduced sediment transport in the Yellow River due to anthropogenic changes. *Nature Geoscience* **9**, 38–41 (2016).
20. Wu, X. *et al*. Stepwise morphological evolution of the active Yellow River (Huanghe) delta lobe (1976–2013): Dominant roles of riverine discharge and sediment grain size. *Geomorphology* **292**, 115–127 (2017).
21. Yu, Z., Wang, X., Han, G., Liu, X. & Zhang, E. Organic and inorganic carbon and their stable isotopes in surface sediments of the Yellow River Estuary. *Biogeosciences Discuss*, https://doi.org/10.5194/bg-2017-353 (2017).
22. Yu, Y. *et al*. Sedimentary trace-element records of natural and human-induced environmental changes in the East China Sea. *Journal of Paleolimnology* **52**, 277–292, https://doi.org/10.1007/s10933-014-9793-3 (2014).
23. Lin, S., Hsieh, I. J., Huang, K.-M. & Wang, C.-H. Influence of the Yangtze River and grain size on the spatial variations of heavy metals and organic carbon in the East China Sea continental shelf sediments. *Chemical Geology* **182**, 377–394, https://doi.org/10.1016/S0009-2541(01)00331-X (2002).
24. Liu, S. M. *et al*. Impacts of human activities on nutrient transports in the Huanghe (Yellow River) estuary. *Journal of Hydrology* **430**, 103–110, https://doi.org/10.1016/j.jhydrol.2012.02.005 (2012).
25. Meyers, P. A. Organic geochemical proxies of paleoceanographic, paleolimnologic, and paleoclimatic processes. *Organic Geochemistry* **27**, 213–250, https://doi.org/10.1016/S0146-6380(97)00049-1 (1997).
26. Brodie, C. R. *et al*. Evidence for bias in C and N concentrations and δ13C composition of terrestrial and aquatic organic materials due to pre-analysis acid preparation methods. *Chemical Geology* **282**, 67–83, https://doi.org/10.1016/j.chemgeo.2011.01.007 (2011).
27. Kaushal, S. & Binford, M. Relationship between C:N ratios of lake sediments, organic matter sources, and historical deforestation in Lake Pleasant, Massachusetts, USA. *J Paleolimnol* **22**, 439–442 (1999).
28. Lamb, A. L., Wilson, G. P. & Leng, M. J. A review of coastal palaeoclimate and relative sea-level reconstructions using δ13C and C/N ratios in organic material. *Earth-Science Reviews* **75**, 29–57, https://doi.org/10.1016/j.earscirev.2005.10.003 (2006).
29. Rumolo, P., Barra, M., Gherardi, S., Marsella, E. & Sprovieri, M. Stable isotopes and C/N ratios in marine sediments as a tool for discriminating anthropogenic impact. *Journal of Environmental Monitoring* **13**, 3399–3408 (2011).

30. Schubert, C. J. & Calvert, S. E. Nitrogen and carbon isotopic composition of marine and terrestrial organic matter in Arctic Ocean sediments: implications for nutrient utilization and organic matter composition. *Deep Sea Research Part I Oceanographic Research Papers* **48**, 789–810 (2001).
31. Shi, H., Wang, X., Xu, M., Zhang, H. & Luo, Y. Characteristics of soil C:N ratio and δ13C in wheat-maize cropping system of the North China Plain and influences of the Yellow River. *Scientific Reports* **7**, 16854 (2017).
32. He, B. *et al*. Sources and accumulation of organic carbon in the Pearl River Estuary surface sediment as indicated by elemental, stable carbon isotopic, and carbohydrate compositions. *Biogeosciences* **7**, 3343–3362, https://doi.org/10.5194/bg-7-3343-2010 (2010).
33. Molinaroli, E. *et al*. Relationships between hydrodynamic parameters and grain size in two contrasting transitional environments: The Lagoons of Venice and Cabras, Italy. *Sedimentary Geology* **219**, 196–207, https://doi.org/10.1016/j.sedgeo.2009.05.013 (2009).
34. Molinaroli, E. *et al*. Sediment grain size and hydrodynamics in Mediterranean coastal lagoons: Integrated classification of abiotic parameters. *Journal of Earth System Science* **123**, 1097–1114, https://doi.org/10.1007/s12040-014-0445-9 (2014).
35. Liu, J. *et al*. Distribution and Budget of Organic Carbon in the Bohai and Yellow Seas. *Advances in Earth Science* (2015).
36. Leng, M. *et al*. In Isotopes in Palaeoenvironmental Research Vol. 10 Developments in Paleoenvironmental Research (ed. MelanieJ Leng) Ch. 04, 147–184 (Springer Netherlands, 2006).
37. Neumann, T., Stögbauer, A., Walpersdorf, E., Stüben, D. & Kunzendorf, H. Stable isotopes in recent sediments of Lake Arendsee, NE Germany: response to eutrophication and remediation measures. *Palaeogeography, Palaeoclimatology, Palaeoecology* **178**, 75–90, https://doi.org/10.1016/S0031-0182(01)00403-5 (2002).
38. Fan, H., Wang, X., Zhang, H. & Yu, Z. Spatial and temporal variations of particulate organic carbon in the Yellow-Bohai Sea over 2002–2016. *Scientific Reports* **8**, 7971, https://doi.org/10.1038/s41598-018-26373-w (2018).
39. Kelts, K. & Hsu, K. J. In *Lakes-chemistry, geology, physics* (ed. Abraham Lerman) Ch. 9, 295–323 (Springer-Verlag 1978).
40. Gireeshkumar, T. R., Deepulal, P. M. & Chandramohanakumar, N. Distribution and sources of sedimentary organic matter in a tropical estuary, south west coast of India (Cochin estuary): A baseline study. *Marine Pollution Bulletin* **66**, 239–245, https://doi.org/10.1016/j.marpolbul.2012.10.002 (2013).
41. Nazneen, S. & Raju, N. J. Distribution and sources of carbon, nitrogen, phosphorus and biogenic silica in the sediments of Chilika lagoon. *Journal of Earth System Science* **126**, https://doi.org/10.1007/s12040-016-0785-8 (2017).
42. Dessandier, P.-A. *et al*. Impact of organic matter source and quality on living benthic foraminiferal distribution on a river-dominated continental margin: A study of the Portuguese margin. *Journal of Geophysical Research-Biogeosciences* **121**, 1689–1714, https://doi.org/10.1002/2015jg003231 (2016).
43. Coynel, A. *et al*. Spatial distribution of trace elements in the surface sediments of a major European estuary (Loire Estuary, France): Source identification and evaluation of anthropogenic contribution. *Journal of Sea Research* **118**, 77–91, https://doi.org/10.1016/j.seares.2016.08.005 (2016).
44. Darrow, E. S., Carmichael, R. H., Calci, K. R. & Burkhardt, W. Land-use related changes to sedimentary organic matter in tidal creeks of the northern Gulf of Mexico. *Limnology and Oceanography* **62**, 686–705, https://doi.org/10.1002/lno.10453 (2017).
45. Sousa, S. H. M. *et al*. Spatial sediment variability in a tropical tide dominated estuary: Sources and drivers. *Journal of South American Earth Sciences* **72**, 115–125, https://doi.org/10.1016/j.jsames.2016.08.004 (2016).
46. Li, D. *et al*. Organic carbon cycling in sediments of the Changjiang Estuary and adjacent shelf: Implication for the influence of Three Gorges Dam. *Journal of Marine Systems* **139**, 409–419, https://doi.org/10.1016/j.jmarsys.2014.08.009 (2014).
47. Wang, H. & Xian, W. Distribution of the total organic carbon of surface sediment and its influence factors in the Yangtze River Estuary. *Marine Sciences* **35**, 24–31 (2011).
48. Zhang, J.-D. *et al*. Distribution and sources of the polycyclic aromatic hydrocarbons in the sediments of the Pearl River estuary, China. *Ecotoxicology* **24**, 1643–1649, https://doi.org/10.1007/s10646-015-1503-z (2015).
49. Ye, F. *et al*. Recent oxygen depletion in the Pearl River Estuary, South China: geochemical and microfaunal evidence. *Journal of Oceanography* **68**, 387–400, https://doi.org/10.1007/s10872-012-0104-1 (2012).
50. Li, D., Liu, X., Liu, Z. & Zhao, X. Variations in total organic carbon and acid-volatile sulfide distribution in surface sediments from Luan River Estuary, China. *Environmental Earth Sciences* **75**, https://doi.org/10.1007/s12665-016-5873-1 (2016).
51. Yu, W., Zhong, S., Pu, X. & Liu, F. Environmental responses of total organic carbon(TOC),acid volatile sulfide (AVS) and heavy metal elements in sediments of Licun Estuary in Jiaozhou Bay. *Journal of Palaeogeography* **11**, 338–347 (2009).
52. Jia, R., Tong, C., Wang, W. & Zeng, C. Organic Carbon Contents and Storages in the Salt Marsh Sediments in the Min River Estuary. *Wetland Science* **6**, 492–499 (2008).
53. Yang, J., Gao, J., Liu, B. & Zhang, W. Sediment deposits and organic carbon sequestration along mangrove coasts of the Leizhou Peninsula, southern China. *Estuarine Coastal and Shelf Science* **136**, 3–10, https://doi.org/10.1016/j.ecss.2013.11.020 (2014).
54. Ramaswamy, V. *et al*. Distribution and sources of organic carbon, nitrogen and their isotopic signatures in sediments from the Ayeyarwady (Irrawaddy) continental shelf, northern Andaman Sea. *Marine Chemistry* **111**, 137–150, https://doi.org/10.1016/j.marchem.2008.04.006 (2008).
55. Yuan, H. M. *et al*. Studies on the regional feature of organic carbon in sediments off the Huanghe River Estuary waters. *Acta Oceanologica Sinica* **23**, 129–134 (2004).
56. Wang, J. & Li, H. Study on chlorophyll and primary production in inshore waters of the Bohai Sea. *Oceanic Fisheries Research* **23**, 23–28 (2002).
57. Zhou, W., Yuan, X., Huo, W. & Yin, K. Distribution of chlorophyll a and primary productivity in the adjacent sea area of Changjiang River Estuary. *Acta Oceanologica Sinica* **26**, 143–150 (2004).
58. Prasad, M. B. K. & Ramanathan, A. L. Sedimentary nutrient dynamics in a tropical estuarine mangrove ecosystem. *Estuarine Coastal and Shelf Science* **80**, 60–66, https://doi.org/10.1016/j.ecss.2008.07.004 (2008).
59. Sun, X. & Turchyn, A. Significant contribution of authigenic carbonate to marine carbon burial. *Nature Geoscience* **7**, 201–204, https://doi.org/10.1038/ngeo2070 (2014).
60. Masse, J. & Montaggioni, L. Growth history of shallow-water carbonates: control of accommodation on ecological and depositional processes. *International Journal of Earth Sciences: Geologische Rundschau* **90**, 452–469, https://doi.org/10.1007/s005310000143 (2001).
61. Dunne, J., Hales, B. & Toggweiler, J. Global calcite cycling constrained by sediment preservation controls. *Global Biogeochemical Cycles* **26**, https://doi.org/10.1029/2010GB003935 (2012).
62. Shen, X., Sun, T., Liu, F., Xu, J. & Pang, A. Aquatic metabolism response to the hydrologic alteration in the Yellow River estuary, China. *Journal of Hydrology* **525**, 42–54, https://doi.org/10.1016/j.jhydrol.2015.03.013 (2015).
63. Kong, D. *et al*. Evolution of the Yellow River Delta and its relationship with runoff and sediment load from 1983 to 2011. *Journal of Hydrology* **520**, 157–167, https://doi.org/10.1016/j.jhydrol.2014.09.038 (2015).

Acknowledgements

This research is supported by the National Key Basic Research Program (2013CB956602), the China Postdoctoral Science Foundation (2018T110067&2016M600059) and the National Natural Science Foundation (41601107), and the Fundamental Research Funds for the Central Universities (312231103).

Author Contributions

X.W. and Z.Y. designed research, Z.Y., X.W., G.H., X.L. and E.Z. analyzed data, Z.Y. and X.W. prepared the manuscript. All authors contributed to the interpretation of results and/or writing.

Additional Information

Competing Interests: The authors declare no competing interests.

Publisher's note: Springer Nature remains neutral with regard to jurisdictional claims in published maps and institutional affiliations.